



## Biosynthesis and Characterization of Zinc Oxide Nanoparticles using Onion Bulb Extract

**N. Tensingh Baliah**

Post Graduate and Research Department  
of Botany, Ayya Nadar Janaki Ammal  
College, Sivakasi, Tamil Nadu, India

**S. Lega Priyatharsini**

Post Graduate and Research Department  
of Botany, Ayya Nadar Janaki Ammal  
College, Sivakasi, Tamil Nadu, India

### ABSTRACT

The wide application of nanoparticles stimulates the need for synthesizing them but, the conventional methods are usually hazardous and energy consuming. This leads to focus on “green synthesis” of nanoparticles which seems to be easy efficient and ecofriendly approach. In this study, the plant mediated synthesis of zinc oxide nanoparticles (ZnO NPs) was carried out using bulb extract of *Allium cepa* as a reducing agent. The optimized nano zinc thus obtained was quantified and characterized using UV-Visible spectroscopy, Fourier Transform Infrared Spectroscopy (FT-IR), X-Ray diffraction, Scanning Electron Microscope (SEM), EDAX and Zeta potential analyses. Further, the synthesized ZnO NPs were tested for antimicrobial activity.

**Keywords:** *Nanoparticles, zinc oxide, biosynthesis, Allium cepa*

### I. INTRODUCTION

Nanotechnology is a emerging field with its application in science and technology for the purpose of manufacturing new materials at nano scale level (Albrecht *et al.*, 2006). Recent advance in the field of nanotechnology, particularly the ability to prepare highly ordered nanoparticles of any size and shape (Sangeetha *et al.*, 2012). Nanotechnology is a multidisciplinary scientific field undergoing explosive development. The nanometer-sized particles offer novel structural, optical and electronic properties that are not attainable with individual molecules or bulk

solids (Anitha *et al.*, 2011). The characters of metal and metal oxide nanoparticles have been of great interest due to their distinctive feature such as catalytic activity, optical, magnetic and electrical properties (Garima *et al.*, 2010). Nanoparticles interaction with biological materials and established a series of nanoparticle / biological interfaces that depend on colloidal forces as well as dynamic biophysicochemical interactions. These interactions lead to the formation of new nanomaterial with control size shape, surface chemistry, roughness and surface coatings.

The use of plants for the synthesis of nanoparticles is novel and provides a cost-effective and environmentally friendly alternative to chemical and physical synthesis. In addition, the use of plants can be easily scaled up for large-scale synthesis without the use of toxic chemicals or the need for high pressures, energy and temperature (Bhainsa *et al.*, 2017). Plant-mediated biosynthesis of zinc oxide nanoparticles has been achieved in *Aloe barbadensis* (Sangeetha *et al.*, 2011), *Physalis alkekengi* (Qu *et al.*, 2011), *Parthenium hysterophorus* (Rajiv *et al.*, 2013), *Zingiber officinale* (Bhuyan *et al.*, 2015), *Azadirachta indica* (Wang *et al.*, 2014), *Ocimum basilicum*, *Medicago sativa* (Nagaiyothi *et al.*, 2013), *Anisochilus carnosus* (Bala *et al.*, 2015), milky latex of *Calotropis procera* and fruit juice of *Citrus aurantifolia* (Samat *et al.*, 2013) *etc.*

It is known that the plant mediated synthesis of ZnO nanoparticles is much safer and environmentally friendly as compared to chemical synthesis. The size of the synthesized ZnO nanoparticles was in the range of 60-70 nm. The larger nanoparticles of ZnO resulted from the agglomeration of smaller nanoparticles. Highly ionic nanoparticulate metal oxides such as zinc oxide nanoparticles are unique in that they can be produced with high surface areas and with unusual crystal structures (Anandraj *et al.*, 2017). Compared to organic materials, inorganic materials such as ZnO possess superior durability, greater selectivity and heat resistance (Padmavathy and Vijayaraghavan, 2008).

## II. MATERIAL AND METHODS

### SYNTHESIS OF ZINC OXIDE NANOPARTICLES

The onion bulbs were washed with sterile distilled water and the outer covering of the bulb was manually peeled off and the fleshy part of the onion was rewashed with sterile distilled water. The onion bulb was cut into small pieces and 10g of bulb was ground using mortar and pestle with distilled water. The extraction was filtered using muslin cloth and then Whatmann No.1 filter paper and used as reducing agent and stabilizer. Zinc nitrate was used as precursor for the synthesis of zinc oxide nanoparticles. For ZnO NPs synthesis, the reaction mixture was prepared by mixing of 10 ml of leaf extract and 90 ml of 1mM zinc nitrate solution in a 250 ml Erlenmeyer conical flask. This mixture was incubated in dark conditions at 37°C. Then, the mixture was centrifuged at 10,000 rpm for 20 minutes. The pellet was taken after centrifugation and air dried. The pellet was used for further studies.

### RECOVERY OF ZnO NANOPARTICLES

The nanoparticles thus obtained were purified by repeated centrifugation at 10000 rpm at 25°C for 10minutes. It was followed by re-dispersion of the pellet in deionized water to get rid of any uncoordinated biological molecules. The process of centrifugation and re-dispersion were repeated with sterile distilled water to ensure better separation of free entities from the nanoparticles.

### CHARACTERIZATION OF ZnO NANOPARTICLES

The synthesized nanoparticles were characterized by UV-Visible spectroscopy, Scanning Electron Microscopy (SEM), Energy Dispersive X-ray Spectroscopy Analysis (EDAX), Fourier Transform Infrared Spectroscopy (FTIR), X-Ray Diffraction (XRD) and Zeta potential analyses.

#### UV-VISIBLE SPECTROSCOPY ANALYSIS

The reduction of pure metal ions was confirmed by measuring the absorption of reaction mixture by UV-Vis Spectrophotometer (UV 1700 SHIMADZU) from 200 to 800 nm (Roy *et al.*, 2013).

#### FOURIER TRANSFORM INFRARED (FTIR) ANALYSIS

FTIR has become an important tool for understanding the involvement of functional groups in interactions between metal particles and biomolecules. FT-IR spectra were recorded at 1 cm<sup>-1</sup> resolution by FTIR spectrophotometer (FTIR-8400S SHIMADZU) using KBr pellet technique (Prathra *et al.*, 2011). The frequency range was measured as wave numbers typically over the range 4000-400 cm<sup>-1</sup>.

#### X-RAY DIFFRACTION (XRD) ANALYSIS

To determine the nature and size of the ZnO nanoparticles, X-ray diffraction (XRD) was performed. The pellet was dissolved in deionized sterile water and washed thrice in the same by centrifugation. The pellet was retained and air dried. The powder from of the sample was coated on the XRD grid, the spectra were recorded 40 kV and a current of 30 mA with CuK $\alpha$  radiation using XRD (Philips PW1050/37 model). The diffracted intensities were recorded from 20°C to 80°at 2 $\theta$  angles. The crystalline nature of synthesized nanoparticles was calculated from the width of the XRD peaks, using the Debye-Scherrer formula ( $D = K\lambda/\beta \cos\theta$ ).

#### SCANNING ELECTRON MICROSCOPY (SEM) ANALYSIS

The synthesized nanoparticles were dispersed in water and the resultant suspensions were homogenized using ultra sonicator for one to two hours. A drop of the nanoparticles suspension was placed on a piece of micro glass slide attached to a metal grid coated with carbon film and dried it gradually at room

temperature. The sample was then sputter coated with gold and visualized with a JEOL JSM-6480 LV SEM to assess the particle size, shape and percentage (Forough and Farhadi, 2010).

### ENERGY DISPERSIVE X-RAY SPECTROSCOPY (EDAX) ANALYSIS

A drop of the nanoparticles suspension was placed on a piece of microglass slide attached to a metal grid coated with carbon film, and dried it gradually at room temperature. X-ray spectrometer (EDAX) operated at an accelerating voltage at 10 KeV. The sample was then sputter coated with gold and visualized with a BRUKER to assess the particle size, shape and percentage of synthesized particles.

### ZETA POTENTIAL ANALYSIS

The supernatant was filtered and then sonicated for 5 minutes. The solution was centrifuged for 15 minutes at 25°C with 5000 rpm and the supernatant was collected. Then, the supernatant was diluted for 4 to 5 times and then set for Zeta-Potential analysis (Mohammed *et al.*, 2014).

### ANTIMICROBIAL ACTIVITY

The ZnO nanoparticles were tested against the bacterial pathogens such as *E.coli* (ATCC25922), *Staphylococcus aureus* (ATCC9144), *Pseudomonas aeruginosa* (ATCC25619) and fungal pathogens *Aspergillus niger* (MTCC 1344) and *Aspergillus flavus* (MTCC 1973). Agar disc diffusion method (Baur *et al.*, 2012) was employed for the study of antimicrobial activity of the synthesized zinc oxide nanoparticles.

### STATISTICAL ANALYSIS

The XRD values were inferred through JCPDS file no 89-3722. Further, the UV-Visible spectrum, FTIR, XRD values were interpreted by using ORIGIN VERSION-8 (data analysis and graphing work space). The data were reported as mean  $\pm$  SE and in the figure parentheses represent the per cent activity.

## III. RESULTS & DISCUSSION

### VISUAL OBSERVATION OF ZINC OXIDE NANOPARTICLES

The synthesized zinc oxide nanoparticles were initially confirmed by visual observation by colour change in the reaction medium. The metal ions were

reduced during the exposure to aqueous extract of onion within 24 hours of incubation period. It was observed that the colour of the reaction medium was changed to pale yellow to pale brown colour (Fig. 1).

### UV-VISIBLE SPECTROSCOPY ANALYSIS

The reduction of zinc oxide ions in the onion extract was further confirmed by UV-Vis Spectrophotometer. UV-Vis absorption spectra of nanoparticles were shown in (Fig. 2). The UV-Vis absorption spectrum of ZnO NPs was as the peak maxima in 354 nm which corresponding to the absorbance of zinc oxide nanoparticles. After incubation period, the colour was changed because of the excitation of Surface Plasmon Vibrations in the ZnO nanoparticle. The reduction of zinc was subjected to analysis by using the UV-Vis Spectrophotometer. Absorption spectra of ZnO NPs formed in the reaction media has absorbance peak at 310nm, broadening of peak indicated that the particles are polydispersed. The frequency and width of the surface plasmon absorption depends on the size and shape of the metal nanoparticles as well as on the dielectric constant of the metal itself and the surrounding medium (Melvin *et al.*, 2009).

The aqueous extract of *Punica granatum* and zinc nitrate solution, the colour of the reaction medium changed rapidly from colour less to brownish yellow. The colour indicated surface plasmon vibration typical of zinc oxide (ZnO) nanoparticles. The maximum intensity at 364nm was observed indicating complete reduction of zinc ions. The UV-Vis optical absorption spectrum of ZnO nanoparticles showed a sharp absorbance at 345 nm, which indicated an almost uniform size of the nanoparticles. However, upon change in particle size or particle shape, a slight shift in the absorption was observed (Guo *et al.*, 2001). The UV-Vis absorption spectrum of ZnO nanoparticles using flower extract of *Nyctanthes arbor-tristis* showed a sharp absorbance at 369 nm (Jamdagni *et al.*, 2016).

### FOURIER TRANSFORM INFRARED SPECTROSCOPY (FTIR) ANALYSIS

FTIR analysis was carried out to identify the biomolecules which were responsible for the reduction of metal ions into ZnO nanoparticles in the presence of onion extract (Fig. 3). The phytochemical found in the onion extract were responsible for the formation of various nanoparticles. The FT-IR spectrum of onion extract showed several absorption

peaks ranged from  $3421\text{cm}^{-1}$  to  $677\text{cm}^{-1}$ . The region of band was phenols, alkanes due to N-H stretching of proteins and O-H stretching,  $>C=O$  stretching of esters, aromatics, ring C-C stretching of phenyl, alkanes, C-O stretch in vibration combined with the ring stretch of phenyl, aliphatic amines, alcohols, carboxylic acids, ester, ether, functional groups mainly from carbohydrate and alkyl halides. FTIR measurements of zinc oxide nanoparticles with onion extract showed the presence of bands at 3438.84, 2925.81, 1633.59, 1383.83, 1122.49, 1104.17 and  $600.78\text{cm}^{-1}$ . These bands were indicating the presence of N-H bend primary amines, C-O stretching alcohols, carboxylic acids, ester and ethers.

FTIR spectrum of ZnO nanoparticles revealed that the peak at  $417.52\text{cm}^{-1}$  was the characteristic absorption of ZnO bond and the broad absorption peak at  $3438\text{cm}^{-1}$  attributed to the characteristic absorption of hydroxyl group (Khan *et al.*, 2011). The FTIR spectrums of ZnO NPs derived from *Corymbia citriodora* leaf extract showed the strong absorption peaks observed at 3300 and  $1620\text{cm}^{-1}$  and were assigned to O-H stretch and N-H bend functional groups. Weaker bands observed at 2955, 777 and  $633\text{cm}^{-1}$  were assigned to  $-C-H$  stretch (alkanes), C-H (aromatics) and  $-C=C-H$  (alkynes). The absorption peaks at 1520 and  $1431\text{cm}^{-1}$  were attributed the C=C bending and C-C stretching of aromatic rings, respectively. The peak at  $1053\text{cm}^{-1}$  assigned to the C-N stretching mode in aliphatic amines. The formation of ZnO NPs may attribute to the chemicals presence in the *C. citriodora* such as citronellal, linalool, catechin, gallic acid, coumaric acid and protocatechuric acid, which acted as reducing agents as well as stabilizing agents (Tamuly *et al.*, 2013).

The FTIR spectrum of ZnO nanoparticles derived from *Ocimum tenuiflorum* showed the fundamental mode of vibration at  $3458.04\text{cm}^{-1}$  which corresponded to the O-H stretching vibration,  $1625.35\text{cm}^{-1}$  which correspond to the N-H bend,  $1418.86\text{cm}^{-1}$  which corresponded to C-C stretching vibration of alcohol, carboxylic acid, ether and ester were confirmed. The band at  $1148.10\text{cm}^{-1}$  corresponds to C-N symmetric stretching vibration and O-H bending of the hydroxyl group at  $3458.04\text{cm}^{-1}$  was observed. The absorption at  $875.23\text{cm}^{-1}$  was due to the formation of tetrahedral coordination of Zn. The bond at  $835.61\text{cm}^{-1}$  was due to the C-Cl stretching vibration. The peak at  $668.29\text{cm}^{-1}$  indicated the stretching vibrations of ZnO

nano particle which was consistent with that reported before (Ravichandrika *et al.*, 2012). From FTIR analysis of leaves extract of *Ocimum tenuiflorum* all functional groups play important role in the preparation of zinc oxide nanoparticles.

Green synthesis of ZnO nanoparticles using *Phyllanthus embilica* stem extract revealed The FT-IR spectra showed the presence of bonds due to O-H stretching around  $3423\text{cm}^{-1}$ . Peak at  $1405\text{cm}^{-1}$  may be assigned to symmetric stretching of the carbonyl side groups in the amino acid residues of the protein molecules. The band at  $1022\text{cm}^{-1}$  was corresponding to C-N stretching vibration of amine. The peak at around  $1340\text{cm}^{-1}$  present in green ZnO signified amide III band of the random coil of protein (Joel and Sheik, 2017).

### X-RAY DIFFRACTION PATTERN ANALYSIS

The various peaks in the XRD pattern could be assigned to the crystalline zinc oxide phase with the hexagonal wurzite structure with the lattice parameters  $a=3.2475\text{nm}$  and  $c=3.2501\text{nm}$ . The XRD pattern showed different intensity peaks in the whole spectrum of  $2\theta$  values ranging from  $20^\circ$  to  $80^\circ$  for the onion. The *Allium cepa* extract-mediated synthesized ZnO nanoparticles were indexed as (100), (002), (101), (102), (110), (103), (200), (112) and (201). The zinc was indexed as (100) and (101). The average crystalline size was determined using Scherrer's equation. The average crystalline size of zinc oxide nanoparticles was 20-100 nm (Fig. 4). Zinc oxide nanoparticles synthesized using *Corymbia citriodora* leaf extract showed the peaks at  $32.1^\circ$ ,  $34.6^\circ$ ,  $36.1^\circ$ ,  $47.7^\circ$ ,  $56.4^\circ$ ,  $63.1^\circ$  and  $68.1^\circ$  and indexed to hexagonal wurzite ZnO (JCPDS 36-1451). Further, no other peaks have been detected in the sample and confirmed the biosynthesis of ZnO NPs owning a high purity. The mean crystalline size was found to be 21 nm (Yuhong Zheng *et al.*, 2017). Biological synthesis of zinc oxide nanoparticles from *Catharanthus roseus* leaf extract showed strong diffraction peaks at 20, 32, 35 and 40 degrees of  $2\theta$  which corresponds to 111, 200, 220 and 311 crystal planes, which were significant agreement with the JCPDS file 36145 ( $a = b = 3.249\text{Å}$ ,  $C = 5.206\text{Å}$ ) and indexed as the hexagonal wurtezite structure of ZnO. High purity and crystallinity of the synthesized ZnO NPs were also confirmed.

## SCANNING ELECTRON MICROSCOPE (SEM) ANALYSIS

The surface morphology of the nanoparticles was characterized using Scanning Electron Microscopy. The onion extract mediated ZnO nanoparticles were found as nano-rod shape (Fig. 5). The biological approach using milky latex of *Calotropis procera* has been used for the first time as a reducing material as well as surface stabilizing agent for the synthesis of spherical-shaped ZnO NPs. The structure, phase and morphology of synthesized product were investigated by the SEM analysis (Sangeetha *et al.*, 2011). Raut *et al.* (2017) done the SEM analysis for zinc oxide nanoparticles synthesized by *Ocimum tenuiflorum* leaf extract. The SEM analysis showed the hexagonal nanoparticle formed with diameter range 11-25nm. ZnO nanoparticles synthesized using *Trifolium pratense* flower extract revealed that SEM images of the ZnO nanoparticles were agglomerated with a particle size ranging from 100–190nm (Dobrucka and Dugaszewska, 2015).

## EDAX ANALYSIS

EDAX analysis is very much useful for further confirmation of presence of nanoparticles. The EDAX analysis showed the confirmative peaks for ZnO NPs. The ZnO nanoparticles were confirmed by typical absorption peak at 1KeV (Fig. 6). Sharma *et al.* (2014) reported that the size of the nanoparticle is more than that calculated from the Debye -Scherrer formula indicating the agglomeration of crystallites in ZnO nanoparticles. The aggregation of particles should have been originated from the large specific surface area and high surface energy of ZnO nanoparticles. The aggregation occurred probably during the process of drying (Raoufi, 2013). The green synthesis of zinc oxide nanoparticles using *Moringa oleifera* leaf extract the strong and weak peaks are observed from Zn and O atom and weak peaks are observed from S, K, C, P, Ca element (Mishra *et al.*, 2015). Biosynthesis and characterization of ZnO nanoparticles using the aqueous leaf extract of *Imperata cylindrica* the EDS spectrum shows the high value of zinc (80.3%) and oxygen (19.65%).

## ZETA POTENTIAL ANALYSIS

Zeta potential measures the potential stability of the nanoparticles in the colloidal suspension. From the Zeta potential analysis, onion extract mediated ZnO nanoparticles carried a charge of  $\pm 26.5$  mV (Fig. 7).

The zeta potential of the biologically synthesized NPs was determined in water as dispersant. The zeta potential was found to be -20 to -30 mV for ZnO nanoparticles. The high negative value approved the repulsion among the particles and thereby increases in stability of the structure of nanoparticles (Jafarirad *et al.*, 2016). It was suggested that the surface of the nanoparticles was negatively charged and dispersed in the medium. The negative value confirms the repulsion among the particles and proves that they are very stable (Anandalakshmi *et al.*, 2016). The biosynthesis of zinc oxide nanoparticles using *Ixora coccinea* leaf extract zeta potential was found to be -49.19 mV (Yedurkar *et al.*, 2016). The synthesis and characterisation of zinc oxide nanoparticles using terpenoid fractions of *Andrographis paniculata* leaves the zeta potential of synthesized ZnO nanoparticles was 17.6 mV.

## ANTIMICROBIAL ACTIVITY

Antimicrobial activity of onion extract mediated zinc oxide nanoparticles were tested against bacterial pathogens such as *E.coli* and *Staphylococcus aureus*, *Pseudomonas aeruginosa* and two fungal pathogens like *Aspergillus niger* and *Aspergillus flavus*. The antibacterial activity (inhibition zone) of zinc oxide nanoparticles was higher against *Pseudomonas aeruginosa* followed by *Staphylococcus aureus* and *E.coli*. In the case of fungal pathogens, the maximum inhibition zone was observed against *A. niger* (Table 1).

Nanoparticles possess the antimicrobial properties against several microorganisms including bacteria, fungi and certain extremophiles (Haeed *et al.*, 2008). The properties of ZnO nanoparticle is strongly influenced by the particle size and mechanism of cell inhibition. The properties include disruption of cell membrane, altering the permeability, electrostatically binding to the cell surface and accumulation of nanoparticle in cytoplasm (Stoimenov *et al.*, 2002). Antimicrobial activity of zinc oxide nanoparticles were known from the very distant past and has many applications in disinfecting medical devices, water purification, and wound healing, creams, lotions and antibacterial creams. The mechanism of action of antimicrobial activity zinc oxide is similar to other nanoparticles, but it acts mostly through destruction of bacterial walls. Zinc oxide nanoparticles have been widely used against Gram-positive and Gram negative bacteria (Emami *et al.*, 2013).

The mechanisms of antibacterial activity of ZnO NPs were direct contact of ZnO NPs with cell walls, resulting in destructing bacterial cell integrity, liberation of antimicrobial ions mainly  $Zn^{+2}$  ions. However, the toxicity mechanism varies in various media as the species of dissolved Zn may change according to the medium components besides the physicochemical properties of ZnO NPs (Yedurkar *et al.*, 2016). Nano-sized ZnO exhibited varying morphologies and showed a significant antibacterial activity over a wide spectrum of bacterial species explored by a large body of researchers. ZnO is currently being investigated as an antibacterial agent in both microscale and nanoscale formulations. ZnO exhibited significant antimicrobial activities when particle size is reduced to the nanometer range, then nano-sized ZnO interacted with bacterial surface and/or with the bacterial core where it entered inside the cell and subsequently exhibited distinct bactericidal mechanisms (Seil and Webster, 2012).

## CONCLUSIONS

The biological production of metal nanoparticles is becoming a very important field in chemistry, biology and materials science. Metal nanoparticles have been produced chemically and physically for a long time; however, their biological production has only been investigated very recently. The biological reduction of metals by plant extracts has been known since the early 1900s; however, the reduction products were not studied. The rapid biological synthesis of zinc nanoparticles using bulb extract of *Allium cepa* provides an environmental friendly, simple and efficient route for synthesis of nanoparticles. The use of plant extracts avoids the usage of harmful and toxic reducing and stabilizing agents. The synthesized nano particles of ZnO are in the range of 20-100 nm. Zinc nanoparticles can exist in ions only in the presence of strong oxidizing substances. The synthesis of ZnO nano particles is still in its infancy and more research needs to be focused on the mechanism of nanoparticle formation which may lead to fine tuning of the process ultimately leading to the synthesis of nanoparticles with a strict control over the size and shape parameters.

## ACKNOWLEDGEMENT

The authors are thankful to the Management and the Principal of Ayya Nadar Janaki Ammal College, Sivakasi, Tamil Nadu, India for providing laboratory facilities to carry out the experiment.

## REFERENCES

1. Albrecht, M. A., Evan, C. W. & Raston, C. L. (2006). Green chemistry and the health implications of nanoparticles. *Green Chemistry*, 3(8), 417-432.
2. Anand Raj, L.F.A. & Jayalakshmy, E. (2017). Biosynthesis and characterization of zinc oxide nanoparticles using root extract of *Zingiber officinale*. *J.Chem*, 31, 51-56.
3. Anandalakshmi, K., Venugobal, J. & Ramasamy, V. (2016). Characterization of zinc oxide nanoparticles by green synthesis method using *Pedaliium murex* leaf extract and their antibacterial activity. *Appl. Nanosci.* 6(2), 399.
4. Anitha, S. Kiruba, D., Singhal, G. (2011). Bhavesh, R., Kunalkasaraiya, M., AshishRajanan, S. & Singh R. Biosynthesis of zinc oxide nanoparticles using *Ocimum sanctum* (Tulsi) leaf extract and screening its antimicrobial activity, *J. Nanopart. Res.*, 13(9), 2981-2988.
5. Bala, N., Saha, S., Chakraborty, M., Maiti, M., Das, S., Basub, R. & Nandyc, P. (2015). Green synthesis of zinc oxide nanoparticles using *Hibiscus subdariffa* leaf extract: Effect of temperature on synthesis, anti-Bacterial activity and anti-diabetic activity. *Int. J. Mol. Sci*, 5, 4993-5003.
6. Baur, R.W., Kirby, M. D. K., Sherris, J. C. & Turck, M. (2012). Antibiotic susceptibility testing by standard single disc diffusion method. *Americ. J. Clin. Pathol.* 45, 493-496.
7. Bhainsa K. C. & Souza, D. (2017). Extracellular biosynthesis of zinc oxide nanoparticles using the fungus *Aspergillus fumigates*. *Biosurfaces*, 47(2), 160-164.
8. Bhuyan, T., Mishra, K., Khanuja, M. & Prasad, R. (2015). Biosynthesis of zinc oxide nanoparticles from *Azadirachta indica* for antibacterial and photocatalytic applications. *Mat. Sci. Semiconduct. Process*, 32, 55-56.
9. Dobruckaand, R. & Dugaszewska, J. (2015). Biosynthesis and antibacterial activity of ZnO nanoparticles using *Trifolium pratense* flower extract. *Saudi J. Biol. Sci.* 23, 517-523.
10. Emami, S., Akya, A., Hossain Zadeh, A. & Barkhordar, S. (2013). Bacterial contamination of traditional ice creams in Kermanshah. *Iran J. Med. Microbiol.* 7(2), 59-62.
11. Forough, M. & Farhadi, K. (2010). Biological and green synthesis of zinc oxide nanoparticles. *Turkish J. Eng. Env. Sci.* 34, 281 - 287.

12. Garima, S., Bhavesh, R., Kunal Kasariya, M., Ashish Ranjan S. & Singh, R. (2011). Biosynthesis of zinc oxide nanoparticles using *Ocimum sanctum* (Tulsi) leaf extract and screening its antimicrobial activity. *J. Nanopart. Res*, 13, 2981-2988.
13. Guo, L., Cheng, X. Y., Yan, Y. J. & Ge, W. K. (2001). Synthesis and optical properties of crystalline polymer-capped ZnO nanorods. *Mat. Sci. Engin*, 16, 123-127.
14. Haeed, A., Hasan, M., Raffi, M., Hussain, F. & Bhatti, T. M. (2008). Antibacterial characterization of zinc oxide nanoparticles against *E.Coli* ATCC-15224. *J. Mater. Sci. Technol*, 24(2), 192-196.
15. Jafarirad, S., Mehrabi, M., Divband, B. & Kosari-Nasab, M. (2016). Biofabrication of zinc oxide nanoparticles using fruit extract of *Rosa canina* and their toxic potential against bacteria: a mechanistic approach. *Mater. Sci. Eng.* 59, 296–302.
16. Jamdagni, P., Poonam Khatri, J. & Rana, S. (2016). Green synthesis of zinc oxide nanoparticles using flower extract of *Nyctanthes arbor-tristis* and their antifungal activity. *J. King. Saud. Univers. Sci.* 3(8), 417-432.
17. Joel, C. & Sheik M. B. (2017). Green synthesis of ZnO nanoparticles using *Phyllanthus embilica* stem extract and their antibacterial activity. *Der. Pharmacia. Lettre.* 8 (11), 218-223.
18. Khan, S. B. and Mohamed, R. (2011). Low temperature growth of ZnO nanoparticles, photocatalyst and acetone sensor. *Talanto*, 85, 943.
19. Melvin Joe, M., Jayochitra, J. & Vijayapriaya, M. (2009). Antimicrobial activity of some common spices against certain human pathogens. *J. Med. Plants Res*, 3, 1134–1136.
20. Mishra, A., Mishra D. K. & Bohra, N. K. (2015). Synthesis and characterization of zinc oxide nanoparticles by *Azadirachta indica* leaves. *Annals Arid Zone* 54(1&2), 43-49.
21. Mohammed, J. Haider & Mehdi, M. S. (2014). Study of morphology and zeta potential analyzer for the zinc oxide nanoparticles. *Int. J. Scienti. Engineer. Res*, 5(7), 381-387.
22. Nagajyothi, P. C., An, T. N. M., Sreekanth, T. V. M., Lee, D. J. & Lee, K. D. (2013). Green route biosynthesis: characterization and catalytic activity of ZnO nanoparticles. *Mat. Lett*, 108(7), 160-163.
23. Padmavathy, N. & Vijayaraghavan R. (2008). Enhanced bioactivity of ZnO nanoparticles-an antimicrobial study. *Sci. Technol. Adv. Mater.* 9: 432-438.
24. Prathra, T. C. N., Chandrasekaran, A.M., Raichur, A. & Mukherjee. (2011). Biomimetic synthesis of zinc oxide nanoparticles by *Citrus limon* (Lemon) aqueous extract and theoretical prediction of particle size. *Colloid. Surf. B: Bioint.* 82, 152-159.
25. Qu, J., Yuan, X., Wang, X. & Shao, P. (2011). Zinc accumulation and synthesis of ZnO nanoparticles using *Physalis alkekengi* L. *Environ. Pollut*, 159, 1783-1788.
26. Rajiv, P., Rajeshwari, S. & Venckatesh, R. (2013). Bio-fabrication of zinc oxide nanoparticles using leaf extract of *Parthenium hysterophorus* L. and its size-dependent antifungal activity against plant fungal pathogens. *Environ. Sci. Technol*, 112, 384-387.
27. Raoufi, D. (2013). Synthesis and microstructural properties of ZnO nanoparticles prepared by the precipitation method. *Renewable Energy*, 50, 932–937.
28. Raut, S., Thorat, P.V. & Thakre, R. (2017). Green synthesis of zinc oxide (ZnO) nanoparticles using *Ocimum tenuiflorum* leaves. *Int. J. Sci. Res.* 4 (5), 1225 – 1228.
29. Ravichandrika, P., Kiranmayi, and Ravikumar, R.V.S. S. N. 2012. Synthesis, characterization and antibacterial activity of ZnO nanoparticles. *Int. J. Pharma. Pharm. Sci.* 4(4), 336-338.
30. Roy, S., Triparna, M., shatarupa, T. & Das, P. (2013). Biosynthesis, characterization and antifungal activity of zinc oxide nanoparticles synthesized by the fungus *Aspergillus foetidus*. *J. Nanometer. Biostruc.* 8, 197–205.
31. Samat, N.A. & Nor, R.M. (2013) Sol-Gel synthesis of zinc oxide nanoparticles using *Citrus Aurantifolia* extracts. *Int. J. Sci. Res.* 39, 545-548.
32. Sangeetha, G., Rajeshwari, S. & Venckatesh, R. (2011). Green synthesis of zinc oxide nanoparticles by *Aloe barbadeneis* Miller. leaf extract: Structure and optical properties. *Mat. Res. Bull*, 46, 2560–2566.
33. Sangeetha, G., Sivaraj, R. & Venckatesh, R. (2012). Green synthesized ZnO nanoparticles against bacterial and fungal pathogens. *Progress in Natural science: Materials International*, 22(6), 693-700.
34. Seil, J. T. & Webster, T. J. (2012). Antimicrobial applications of nanotechnology: methods and literature. *Int. J. Nanomed*, 7(2), 2767–2781.

35. Sharama, G., Jasuja, N. D., Ali, M. I. & Joshi, S. C. (2014). A review on nanomedicinal and nanosensing potential of nanoparticles. *Int. J. Biol. Chem*, 8 (2), 58-84.
36. Stoimenov P. K., Klinger R. L., Marchin G. L., & Klabunde K. J. 2002. Metal oxide nanoparticles as bactericidal agents. *Langmuir* 18(17), 6679- 6686.
37. Tamuly, M., Hazarika, S., Borah, M. R., Das & M. P. Boruah. (2013). *In situ* biosynthesis of Ag, Au and bimetallic nanoparticles using *Piper pedicellatum*: Green chemistry approach. *Colloids Surf. B Biointerf.* 102, 627–634.
38. Wang, X.X., Wu, L., Zhou, P., Li, C., Zhao, L.B., An. W. and Chen, Y. (2014) Effect of ZnO nanoparticles on *Medicago sativa* at the germination stage. *Appl. Mechan. Mat.* 665, 583-586.
39. Yedurkar, S., Maurya, C. & Mahanwar P. (2016). Biosynthesis of Zinc Oxide nanoparticles using *Ixora coccinea* leaf extract - a green approach. *Open J. Syn. Theo. Appli.* 5, 1-14.
40. Yuhong Zheng, Li Fu, Fuigui Han, Aiwu Wang, Wen Cai, Jinping Yu, Jun Yang & Feng Peng (2017). Green biosynthesis and characterization of zinc oxide nanoparticles using *Corymbia citriodora* leaf extract and their photocatalytic activity. *Green Chem. Lett. Rev.* 8(2), 59–63.

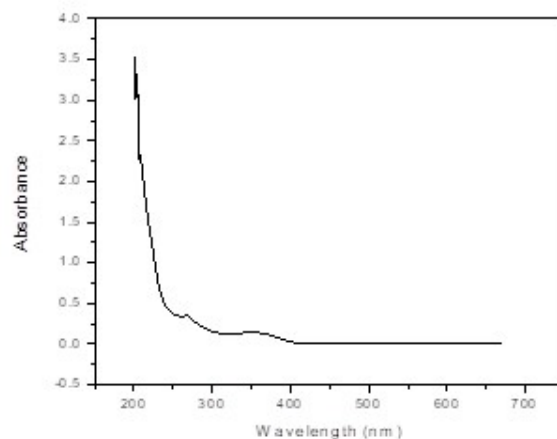


**Fig. 2: UV-Visible spectrum of Zinc oxide nanoparticles**

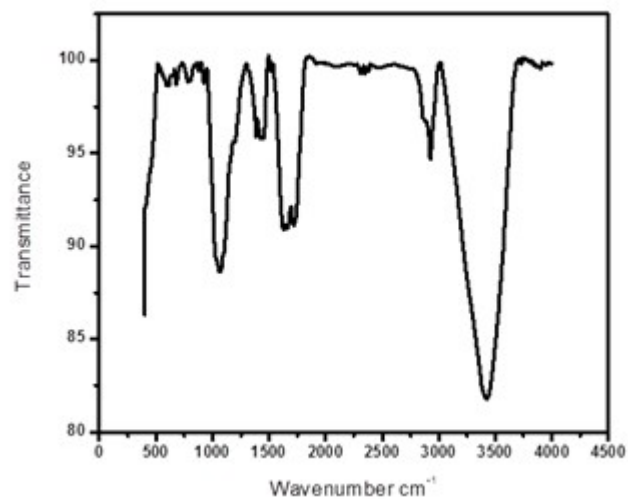
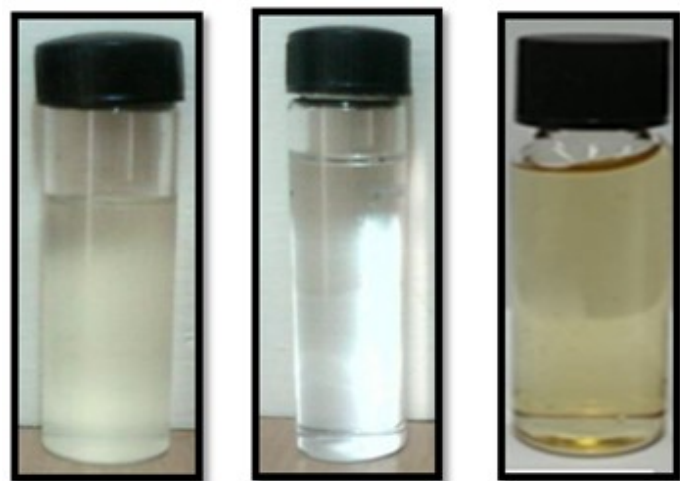


**Fig. 3: FTIR spectrum of Zinc oxide nanoparticles**



**Onion Extract**

**ZnNO<sub>3</sub>**

**ZnO NPs**

**Fig. 1: Visual observation of synthesis of Zinc oxide nanoparticles**

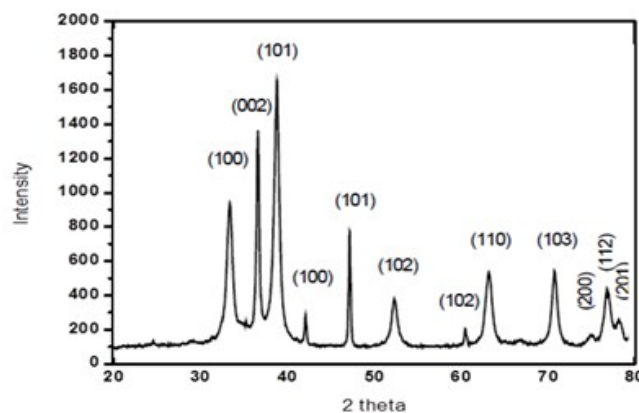


**Fig. 4: XRD spectrum of the Zinc oxide nanoparticles**

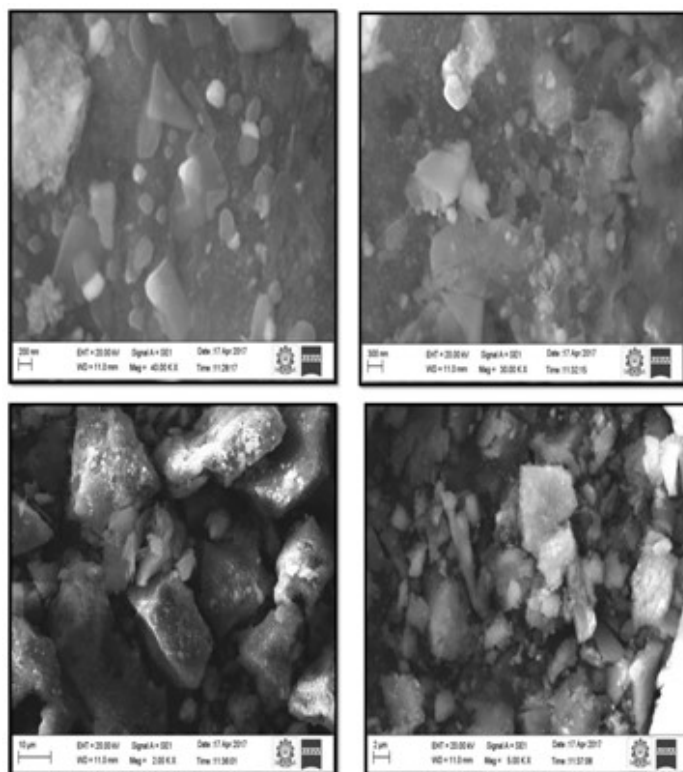


Fig. 5: SEM micrograph of Zinc oxide nanoparticles at different magnifications

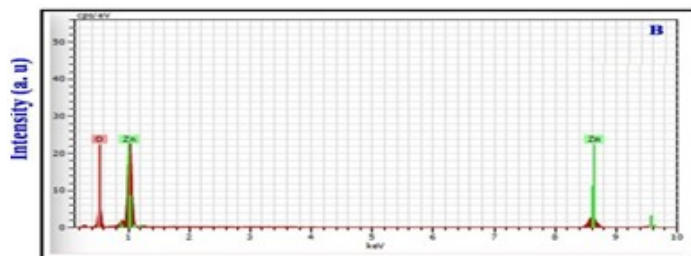


Fig. 6: EDAX spectrum of Zinc oxide nanoparticles

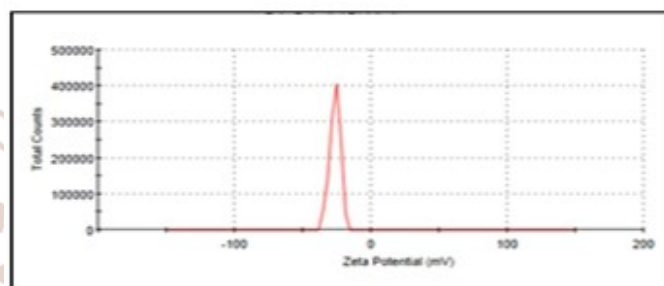


Fig. 7: Zeta potential spectrum of Zinc oxide nanoparticles

Table 1: Antimicrobial activity of Zinc Oxide nanoparticles

Microorganism	Diameter of inhibition zone (mm)	
	Onion Extract	Zinc oxide nanoparticles
<i>E. coli</i>	0.91 ±0.02	1.9 ±0.04
<i>P. aeruginosa</i>	1.72 ±0.03	2.5 ±0.04
<i>S. aureus</i>	1.6 ±0.04	2.4 ±0.07
<i>A. niger</i>	1.2 ±0.09	2.9 ±0.03
<i>A. flavus</i>	1.6 ±0.09	2.2 ±0.02